CHEMBIOCHEM

DOI: 10.1002/cbic.200900030

Pyrazine Arotinoids with Inverse Agonist Activities on the Retinoid and Rexinoid Receptors

José García,[a] Harshal Khanwalkar,[b] Raquel Pereira,[a] Cathie Erb,[b] Johannes J. Voegel,[c] Pascal Collette,[c] Pascale Mauvais,[c] William Bourguet,[d] Hinrich Gronemeyer,*[b] and Ángel R. de Lera*[a]

Heterocyclic arotinoids derived from central-region dihalogenated pyrazine scaffolds have been synthesized by consecutive halogen and/or position-selective palladium-catalyzed cross-coupling reactions. Pyrazines were further functionalized as alkyl ethers or methylamines prior to the last Pd-catalyzed reactions. Transient transactivation studies with the retinoic acid receptor (RAR) α, β, and γ subtypes and with retinoid X receptor (RXR) α revealed distinct agonist, antagonist, and inverse agonist activities for these compounds. Of interest are the RARα,β-selective inverse agonists with pyrazine acrylic acid structures, in particular **14c**, which is RARβ-selective, and **14d**, a pan-RAR/RXR inverse agonist with more affinity for the RAR subtypes that enhance the interaction of RAR with cognate corepressors.

Introduction

Retinoic acid receptors (RARs) and retinoid X receptors (RXRs) [1,2] are members of the nuclear receptor superfamily and act as ligand-dependent transcription factors.[3] The modulation of RARs and RXRs by retinoids contributes to the well-known biological activities of these small-molecule ligands on cell growth and differentiation, carcinogenesis, homeostasis, and development.[4] As a consequence, RAR and RXR ligands (also termed rexinoids) have become important drugs not only for cancer therapy and prevention,[5] but also for the treatment of metabolic diseases through modulation of the heterodimers formed between RXR and other nuclear receptors.[6–9]

Comprehensive structural information is available on both RARs and RXRs including the particular features of the RARα, β, and γ subtypes.[1,2] The ligand-binding domain of RAR defines a linear I-shaped pocket, which can easily accommodate both all-*trans*-retinoic acid **1** and 9-*cis*-retinoic acid **2** (Scheme 1) with the latter ligand adopting a *trans*-like conformation.[10] On the contrary, RXR harbors an L-shaped ligand-binding pocket with a shorter maximal length.[11] To bind RXR, natural retinoids must adopt a sharp bend or a twist of the side-chain, which is feasible for the 9-*cis* but unlikely for the more extended all-*trans* isomers.

Whereas all of the amino acids in contact with the ligand in the ligand-binding domain (LBD) are the same in the RXR subtypes, there are differences in the identity of three amino acids in contact with the ligand in the RAR subtypes. Extensive studies on ligand specificity have provided a reasonable understanding of the structural principles that govern subtype selectivity, and therefore structure-guided design of novel subtype-selective RAR ligands is now feasible.[12]

A series of synthetic derivatives, termed arotinoids[13] replace some of the polyene double bonds of the classical retinoids by arenes. Compared to the flexibility of natural retinoids, these analogues are forced to adopt defined shapes, which are pri-

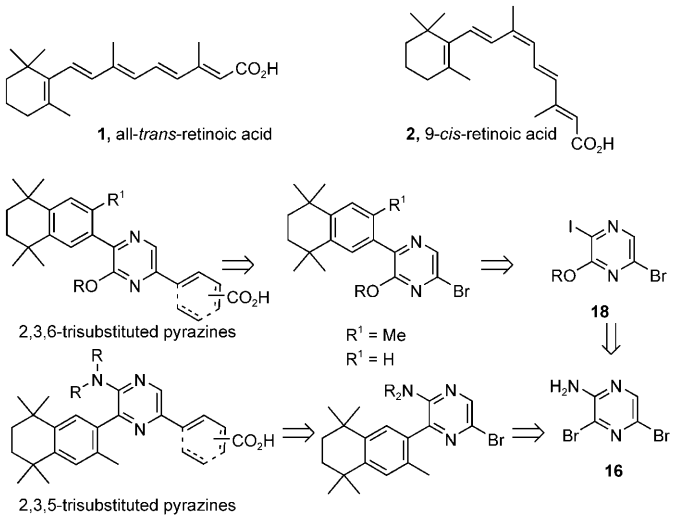

Scheme 1. Structure of natural retinoids (**1**, **2**) and the pyrazine arotinoids that are reported in this work, together with the retrosynthetic analysis.

[a] *J. García, Dr. R. Pereira, Prof. Dr. Á. R. de Lera*
Departamento de Química Orgánica, Universidade de Vigo
Lagoas-Marcosende, 36310 Vigo (Spain)
Fax: (+34) 986811940
E-mail: qolera@uvigo.es

[b] *H. Khanwalkar, C. Erb, Dr. H. Gronemeyer*
Department of Cancer Biology
Institut de Génetique et de Biologia Moléculaire
et Cellulaire (IGBMC)/CNRS/INSERM/ULP
BP 163, 67404 Illkirch (France)
Fax: (+33) 3-88-65-3437
E-mail: hg@igbmc.fr

[c] *Dr. J. J. Voegel, Dr. P. Collette, Dr. P. Mauvais*
GALDERMA R&D, Les Templiers
2400 Route des Colles, 06902 Sophia-Antipolis (France)

[d] *Dr. W. Bourguet*
Université de Montpellier, CNRS, UMR5048
Centre de Biochimie Structurale (CBS) and INSERM, U554
34090 Montpellier (France)

marily determined by the substitution pattern of the arenes or heteroarenes, in particular in cases in which these fragments are the central linkers between the hydrophobic and polar termini of the retinoid skeleton. For example, although the *para*-substituted benzene derivatives are linear and the *meta* isomers of the extended retinoid skeletons are inherently bent, these two families of ligands are likely to selectively target either RAR or RXR, respectively.[14]

The beneficial effect of heteroatoms on the physicochemical properties of retinoids has been frequently claimed.[15] Notably, heterocyclic and heteroaryl scaffolds have replaced the hydrophobic ring and the polar terminus of the retinoid skeleton.[12] Heteroaromatic rings have been included as central retinoid linkers less frequently.[14,16–19] We therefore set out to design, synthesize and assess the ligand binding of a collection of retinoids that have a pyrazine heterocycle as a central connecting unit. To meet the structural requirements for RAR or RXR selectivity, we focused on two series of positional isomers that are derived from 2,3,6- and 2,3,5-trisubstituted pyrazines (Scheme 1). The relevance of the heterocyclic ring on the design is reinforced by its synthetic role as a central scaffold to which the flanking fragments are attached. The development of contemporary methods for C–C bond formation by using Pd-catalyzed reactions[20] called for the multiple functionalization of the heteroaryl ring with halogens. We describe herein the implementation of these principles to the preparation and biological evaluation of a family of retinoids and rexinoids with a central pyrazine ring.

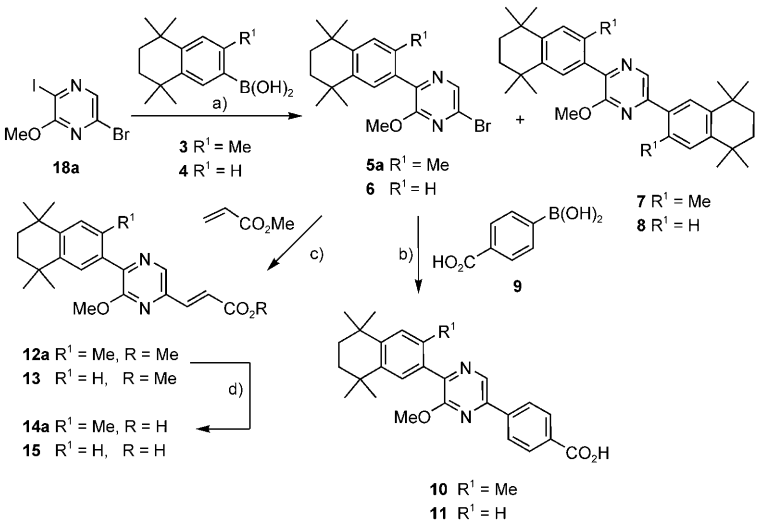

Scheme 2. Reagents and conditions: a) $Pd(PPh_3)_4$, aq Na_2CO_3, MeOH, benzene, 70 °C, 16 h (**5a**, 81%; **7**, 2%; **6**, 74%; **8**, 10%). b) $Pd(PPh_3)_4$, **9**, aq Na_2CO_3, MeOH, dioxane, 130 °C, 15 h (**10**, 75%; **11**, 76%). c) $Pd(OAc)_2$, nBu_4NCl, $NaHCO_3$, 4 Å MS, DMF, 70 °C, 17 h (**12a**, 94%; **13**, 86%). d) LiOH·H_2O, THF/H_2O (1:1), 25 °C, 2 h (**14a**, 99%; **15**, 77%).

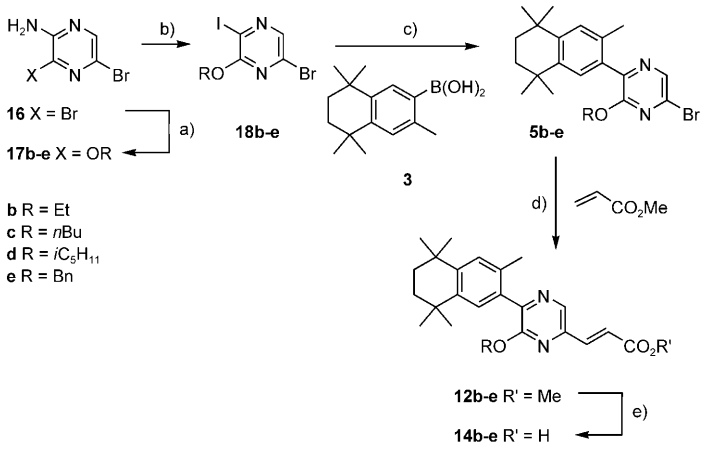

Scheme 3. Reagents and conditions: a) ROH, NaH, THF, MW (200 W), 15 min (**17b**, 60%; **17c**, 75%; **17d**, 70%; **17e**, 75%). b) aq HI, $NaNO_2$, CH_3CN, H_2O, 60 °C, 15 h (**18b**, 50%; **18c**, 66%; **18d**, 45%; **18e**, 50%). c) $Pd(PPh_3)_4$, aq Na_2CO_3, MeOH, benzene, 70 °C, 16 h (**5b**, 76%; **5c**, 48%; **5d**, 51%; **5e**, 63%). d) $Pd(OAc)_2$, nBu_4NCl, $NaHCO_3$, 4 Å MS, DMF, 70 °C, 17 h (**12b**, 94%; **12c**, 77%; **12d**, 87%; **12e**, 89%). e) LiOH·H_2O, THF/H_2O (1:1), 25 °C, 2 h (**14b**, 64%; **14c**, 95%; **14d**, 99%; **14e**, 95%).

Results

A concise and convergent synthetic scheme (Scheme 1) for the preparation of the novel ret(x)inoids was conceived based on the availability of dihalogenated pyrazines **16** and **18**, which were easily synthesized from commercially available 2-aminopyrazine.[21,22] Two consecutive Pd-mediated cross-coupling reactions were planned, the success of which would rely on the anticipated differential reactivity of the halogens on the heterocycle. Previous studies had demonstrated halogen and position-selective reactions of dihalopyrazines similar to **16** and **18**.[22–26]

The retinoids with linear substitution of the pyrazine core were derived from 2-alkoxy-6-bromo-3-iodopyrazines **18** (Scheme 2 and 3). The Suzuki coupling of model dihalopyrazine **18a** and aryl boronic acids **3** and **4** took place at 70 °C in the presence of $Pd(PPh_3)_4$ and aqueous Na_2CO_3.[22] The desired products **5a** and **6** were obtained in good yield, but were accompanied by small amounts of the bis-coupled derivatives **7** and **8** (2% and 10% yield, respectively; Scheme 2). Use of lower temperatures led to partial recovery of starting material and reduced yield of the desired arylpyrazine. A Suzuki coupling with 4-carboxyphenylboronic acid and a Heck reaction with methyl acrylate followed by saponification allowed us to incorporate two of the most common polar retinoid endgroups, a benzoic acid and an acrylic acid, respectively. Due to the electron-withdrawing nature of the carboxylic acid, the coupling with boronic acid **9** to afford arotinoids **10** and **11** required forcing reaction conditions ($Pd(PPh_3)_4$, aqueous Na_2CO_3, MeOH/dioxane, 130 °C, 15 h). Only by using the Jeffery modification of the Heck reaction, in the presence of nBu_4NCl and under strictly anhydrous conditions, could **5a** and **6** efficiently react with methyl acrylate to produce the desired product (**12a** and **13**).[27] Hydrolysis (LiOH·H_2O) afforded carboxylic acids **14a** and **15** (Scheme 2).

A similar synthetic sequence was used in the preparation of novel cinnamic acids that incorporate bulkier alkoxy substituents on the pyrazine ring. Treatment of 2-amino-3,5-dibromopyrazine **16** with the sodium salts (prepared in situ) of a series of alcohols in anhydrous THF under microwave irradiation[28,29] afforded alkyl ethers (**17b**–**e**) in moderate-to-good yields (Scheme 3). Conversion of the amino to the iodopyrazines (compounds **18b**–**e**) relied on the formation of the intermediate diazonium salt and was affected by treatment with aqueous HI in the presence of $NaNO_2$. The differential reactivity of the halogens[22] allowed for the application of sequential Pd-catalyzed reactions with aryl boronic acid **3** and methyl acrylate, as described for the methoxy analogue **12a** (Scheme 2).[27] The Suzuki reaction to afford alkyl ethers **5b**–**d** could not be taken to completion under the optimized reaction conditions, and considerable amounts of starting material were recovered (**18b**, 18%; **18c**, 30%; **18d**, 26% respectively). The Heck reaction provided good-to-excellent yields of the final pyrazine arotinoids **12b**–**e**. Finally, saponification of esters **12b**–**e** yielded the desired acids **14b**–**e**.

Lastly, to construct central-region-pyrazine arotinoids with a bent overall shape, we selected the position-selective Suzuki reaction of 2-amino-3,5-dibromopyrazine **16**[26,30–32] and boronic acid **3** to prepare **19** (81%). A subsequent Suzuki coupling with 4-carboxyphenylboronic acid led to **20** in low yield (39%, Scheme 4); this low yield was due to the compound's instability during the purification step. In addition, a Heck reaction of bromopyrazine **21** (obtained by methylation of the amino group of **19** in 93% yield) produced compound **22** in 66% yield, which was finally saponified to **23** (96%).

We used a reporter assay with a genetically engineered HeLa cell line[33] that had been stably cotransfected with a chimeric receptor construct and the cognate reporter gene to evaluate the effects of the described retinoids on RARα, RARβ, RARγ, and RXRα-mediated transactivation. (There are no differences among the amino acid residues that constitute the ligand-binding pockets of the RXR subtypes). Two types of cellular reporter systems were used that gave virtually identical results on the transactivation characteristics and potency of the various ligands. Both systems contained a stably expressed receptor chimera with a heterologous DNA-binding domain, and the cognate luciferase reporter gene (see the Experimental Section).

For the description of the activity of RAR ligands we have adopted the Monod, Changeux and Wyman model,[34] which assumes that in the absence of ligand, receptors are in equilibrium between the inactive or resting state (**R**) and the active state (**A**). A constant is then determined to measure the affinity of the molecule for each state of the receptor.[35] K_{dA} represents the dissociation constant of the ligand for the receptor in the active state and K_{dR} represents the dissociation constant of the ligand for the receptor in the resting state. The apparent K_d (K_{dapp}) normalizes the values due to the fluctuations of the basal activity and receptor expression levels. To determine these constants, "crossed curves" of the test product (ten concentrations) against a reference agonist (seven concentrations) are performed in 96-well plates. In each well, the cells are in contact with a concentration of the test product and a concentration of the reference agonist. These experimental crossed curves are then compared to theoretical curves obtained by modeling the mathematical equations governing the equilibrium between the two receptor states in the presence of various ligands (see the Experimental Section). A K_{dR}/K_{dA} ratio that is significantly larger than two is characteristic of full agonists (RXRα, RARα and RARβ full agonists, $K_{dR}/K_{dA} \geq 200$; RARγ full agonists, $K_{dR}/K_{dA} \geq 50$ (RARγ presents a higher basal activity, which results in a lower K_{dR}/K_{dA} ratio for full agonists). A K_{dR}/K_{dA} ratio equal (or very close) to one (0.5 to 2) is characteristic of antagonists, and a K_{dR}/K_{dA} ratio lower than 0.5 describes inverse agonists. Note that the term "inverse agonist" used here is deduced from transactivation studies (see the Experimental Section); these data do not allow one to draw conclusions about the underlying mechanistic basis, which might or might not be related to the ability of certain inverse agonists to stabilize corepressor–receptor complexes (vide infra).[36]

All compounds were tested for their RARα,β,γ activity and RXRα activity. The K_{dA} and K_{dR} values of the ligand of interest resulting in the best fit between experimental and theoretical curves are reported in Table 1.

In general, the pyrazine-based arotinoids are inactive on RARγ but are good RARα,β inverse agonists, in particular the pyrazine acrylic acid derivatives (**14a**–**e**). The length and size of the alkoxy groups has a minor, but noticeable influence on the activity levels, with **14b** and **14c** (OR = OEt and O*n*Bu, respectively) showing high affinity, and the latter in particular being a more selective RARβ inverse agonist. Compound **14b**, which exhibits the same affinity for RARα and RARβ, is nonetheless able to reduce the basal activity of RARβ in preference to RARα. The benzoic acid derivatives **10** and **15** are a low-affinity inverse agonist and antagonist, respectively.

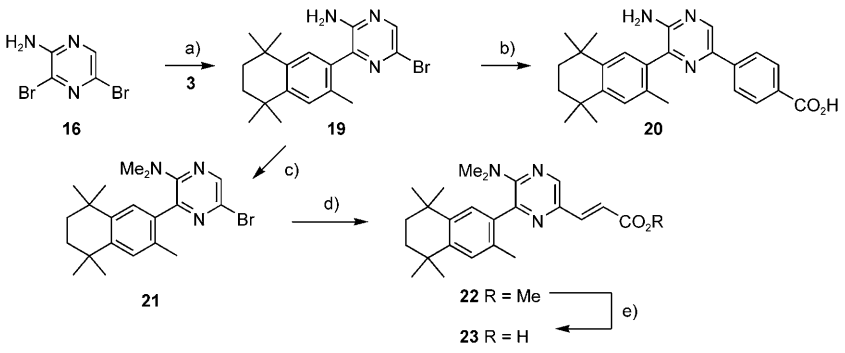

Scheme 4. Reagents and conditions: a) **3**, $Pd(PPh_3)_4$, aq Na_2CO_3, MeOH, benzene, 70 °C, 16 h (81%). b) $Pd(PPh_3)_4$, aq Na_2CO_3, MeOH, dioxane, 130 °C, 15 h (39%). c) NaH, MeI, DMF, 15 min. 25 °C (93%). d) $Pd(OAc)_2$, nBu_4NCl, $NaHCO_3$, 4 Å MS, DMF, 70 °C, 17 h (66%). e) $LiOH \cdot H_2O$, THF/H_2O (1:1), 25 °C, 2 h (96%).

Table 1. Transcriptional activities of pyrazine arotinoids.[a]

Compd. No.	RARα K_{dapp} [nM]	RARα K_{dR}/K_{dA}	RARβ K_{dapp} [nM]	RARβ K_{dR}/K_{dA}	RARγ K_{dapp} [nM]	RARγ K_{dR}/K_{dA}	RXRα K_{dapp} [nM]	RXRα K_{dR}/K_{dA}
11	1000	10	500	5	200	2	n.a.[b]	n.a.
10	250	0.2	500	0.2	500	1	n.a.	n.a.
15	2000	1	2000	1	n.a.	n.a.	n.a.	n.a.
14a	30	0.1	10	0.1	200	1	n.a.	n.a.
14b	2	0.1	2	0.02	1000	0.1	n.a.	n.a.
14c	15	0.01	4	0.01	500	0.3	n.a.	n.a.
14d	8	0.02	4	0.05	1000	0.1	2000	0.2
14e	1	0.01	1	0.01	1000	0.2	n.a.	n.a.
20	250	500	15	500	500	100	2000	1
23	n.d.[c]	n.d.	n.d.	n.d.	n.d.	n.d.	500	250

[a] For RXRα, RARα and RARβ values of $K_{dR}/K_{dA} \geq 200$ indicate full agonists and lower values indicate partial agonists; for RARγ values of $K_{dR}/K_{dA} \geq 50$ indicate full agonists and lower values indicate partial agonists. For all subtypes values of $K_{dR}/K_{dA} \leq 2$ and ≥ 0.5 indicate antagonists, and values of $K_{dR}/K_{dA} < 0.5$ indicate inverse agonists. [b] n.a. not active. [c] n.d. not determined (experimental data do not fit the theoretical model).

Compound **20** with an amine substituent is a full pan-agonist with some RARβ selectivity. Pyrazine arotinoid **23** is active on RARs but concomitant RXR activity precluded the exact determination of the dissociation constant.

To directly address the question of whether the presently observed inverse agonism could be due to altered corepressor interaction, we performed transient two-hybrid experiments using recombinants that express fusions of the GAL4 DNA-binding domain (DBD) and the corepressors NCoR or SMRT as transcription activators of a cotransfected cognate 17-mer globin promoter–luciferase reporter gene. In addition, a second fusion protein comprising a RAR ligand-binding domain (LBD) that is linked to the acidic activation domain of VP16 is coexpressed. In the absence of ligand the corepressor interacts with the RAR LBD and the VP16 transcription activation is tethered to the GAL4 DBD; this results in the activation of luciferase expression (Figure 1, lane EtOH). Agonists dissociate corepressors and this leads to a decreased luciferase expression (lane TTNPB). Provided that an inverse agonist stabilizes the interaction between RAR LBD and the corepressor, increased luciferase expression is expected. This is indeed the case for both **14d** and **14e**, which increase luciferase reporter activity by about 50 to 100% for both the RARα and RARβ LBDs (lanes **14d**, **14e**). A similar stabilization of corepressor binding is seen also with the RXR LBD (data not shown). It is worth pointing out that the latter two inverse agonists enhance the binding of NCoR and SMRT similarly, but known inverse agonist BMS493 (compound **27**, Figure 2) interacts differently with the two corepressors and stabilizes predominantly the NCoR binding (lanes 493). Together these results strongly support the notion that the observed inverse agonism of **14d** and **14e** is due to allosteric effects on the RAR LBD and this results in stabilization of corepressor interaction.

Although in general the pyrazine-based arotinoids with a linear shape do not bind to RXRα (with the exception of **14d**), those analogues with a bent shape seem to have a potential for binding to RXRα: compound **23** is an agonist (500 nM and strong RAR over-activation through synergy), whereas **20** and **14d**, which has an isoamyl ether as substituent, are antagonist and inverse agonist, respectively. The profile of **14d** is unique, because it is at the same time an inverse agonist of RXRα and of all RAR subtypes.

We have described that fluorescence anisotropy measurements of a fluorescein moiety that had been attached selectively to the C terminus of RXR helix H12 of a RARα–RXRα LBD heterodimer allows us to correlate the pharmacological activity of RXR modulators and their impact on the structural dynamics of the activation helix H12.[37] As shown in Figure 3A, compounds **20** and **14d** increase the mobility of helix H12 as revealed by the decreased anisotropy values that were measured in the presence of these ligands as compared with those that were obtained with the full-agonist **24** (Figure 2). However, this destabilizing effect is smaller than that observed with the full antagonist **25** (UVI3003); this suggests a partial antagonism/inverse agonism behavior of ligands **20** and **14d**. Addition of increasing concentrations of a 13-residue peptide corresponding to the nuclear receptor box two region of the transcriptional intermediary factor two (TIF-2 NR2) led to an increase of anisotropy values; this indicates holo-H12 stabilization (Figure 3B); however, the peptide effect greatly varied according to the bound ligand. In the presence of the agonist **24**, low TIF-2 NR2 concentrations suffice to fully stabilize holo-H12, whereas with compound **14d**, the fluorescence anisotropy values remain very low; this demonstrates the strong antagonist/inverse agonist nature of this compound. Ligands **20** and **25** display intermediary profiles with a slow increase of anisotropy values upon peptide addition. However, even the highest dose of TIF-2 NR2 failed to stabilize holo-H12, and accordingly UVI3003 (**25**) has been functionally characterized as a full RXR antagonist.[37,38] Based on these dynamic data, compound **20** can be classified as a weaker antagonist, in line with the above transactivation study.

Discussion

Klein et al. reported the first examples of inverse agonism in the nuclear receptor field.[39] The series of acetylenic arotinoids with small substituents at the C1 position of the aryl dihydronaphthalene ring (**26**, Figure 2) did not transactivate the RARs, but instead they functioned as effective antagonists. Whereas the compounds with the smaller substituents (**26**, R = H, F) behaved as RAR-neutral antagonists, analogues with larger substituents (**26**, R = CH_3, CF_3, Cl) repressed even the basal activity of RARs and were thus classified as inverse agonists. Functional analysis in cultured human keratinocytes revealed the distinct mode of action of these ligands in modulating MRP-8 expression.[39]

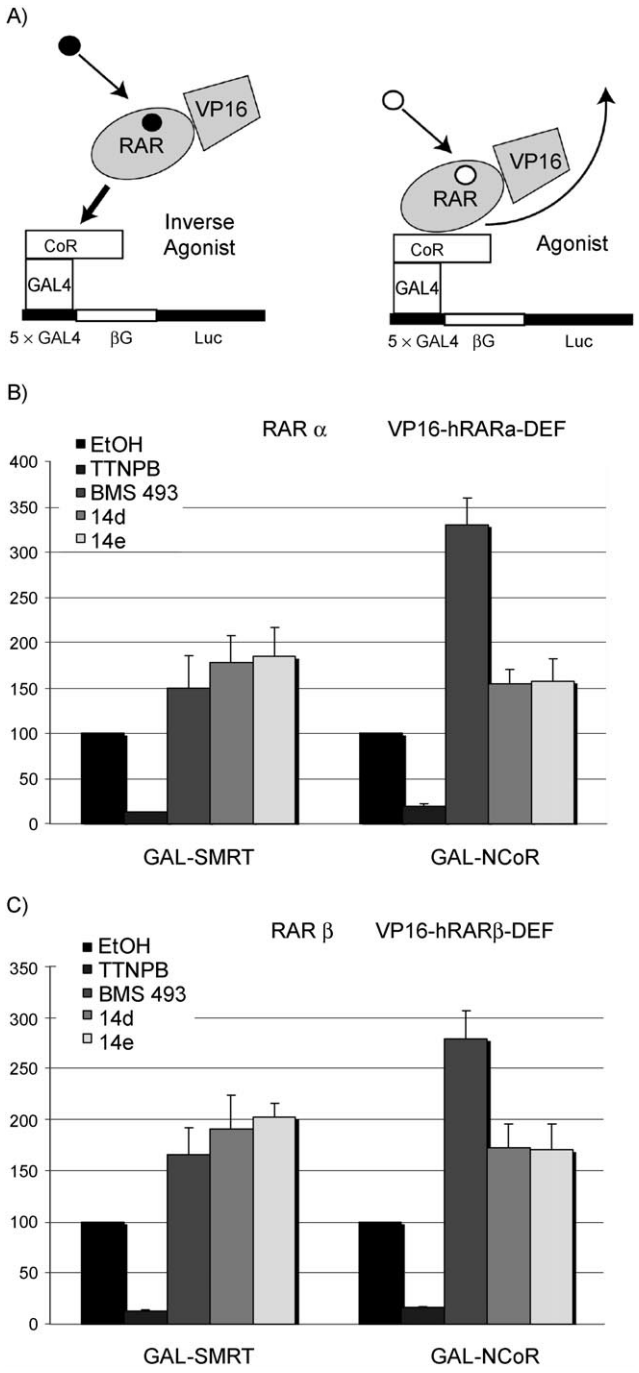

Figure 1. A) Mammalian two-hybrid assays, with (17 m)5×-G-Luc reporter and GAL-NCoR or GAL-SMRT as bait and VP16-RAR as prey, were performed in HeLa cells. B) RARα; C) RARβ.

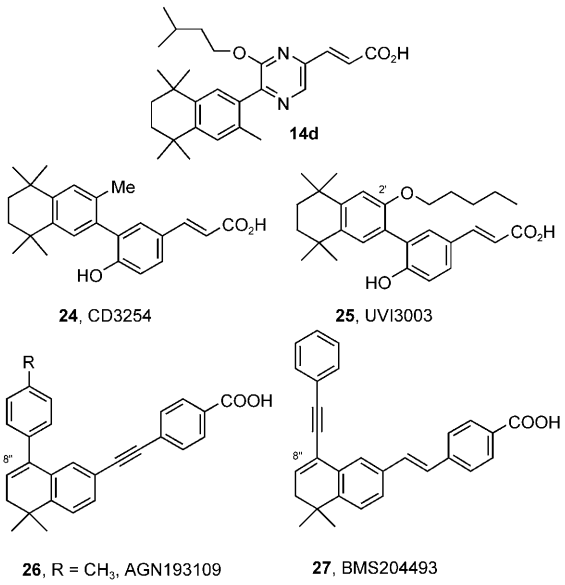

Figure 2. RXR agonist CD3254 **24** and RXR antagonist UVI3003 **25** that were used as control in the fluorescence anisotropy studies and structures of the RAR/RXR inverse agonists.

The active repression (or inverse agonism) induced by certain ligands in the absence of added RAR agonist has been re-examined in the light of the knowledge that has been gained in the last few years about the principles of transcriptional modulation[40] by nuclear receptors and retinoid receptors in particular.[12,41,42] In the absence of a ligand the functional RAR–RXR heterodimer expresses a surface on RAR that allows interaction with corepressors (CoRs), which in turn recruit histone deacetylases (HDACs) thereby establishing HDAC–CoR complexes that might contain additional factors and collectively act as epigenetic silencing machineries.[40,43–46] The addition of RAR agonists induces a conformational switch of the LBD mediated primarily by the repositioning of the amphipathic helix H12. This ligand-induced conformational change affects the surfaces involved in both coactivators (CoA) and CoR interaction.[41,42,47] As a result, CoR–HDAC complexes are released, and positively acting complexes that contain coactivators of the p160 class and their associated histone acetyltransferases (HATs, such as the CREB-binding protein CBP) are recruited. This large protein complex induces local histone acetylation and chromatin decondensation over the target gene promoter regions, thus preparing the gene for subsequent interaction with the chromatin-remodeling and transcription-activating machineries. Neutral antagonists, on the other hand, not only induce dissociation of CoRs but also decrease the affinity of co-activator interaction below the level that is seen with the non-liganded receptor. Inverse agonists, such as AGN193,109 **26** and BMS204,493 **27** (Figure 2) in turn repress the basal activity of RARs by strongly enhancing the interaction with nuclear CoRs in the context of the heterodimer.[36,39]

From the structural point of view, inverse retinoid agonists are more similar to neutral antagonists than to agonists, as shown by the series of antagonists/inverse agonists described in the literature (Figure 2).[48,12] Acetylene and stilbene arotinoids such as **27** and **26** are endowed with antagonist properties when large substituents are added to the C8′′ position of the dihydronaphthalene hydrophobic core structure.[49] These large groups are known to interfere with the repositioning of H12 that is associated to the conformational switch triggered by the agonist.[50,51]

As a complementary structural approach, we designed novel arotinoids that share a central trisubstituted pyrazine ring and differ in the connections to the hydrophobic and polar end-

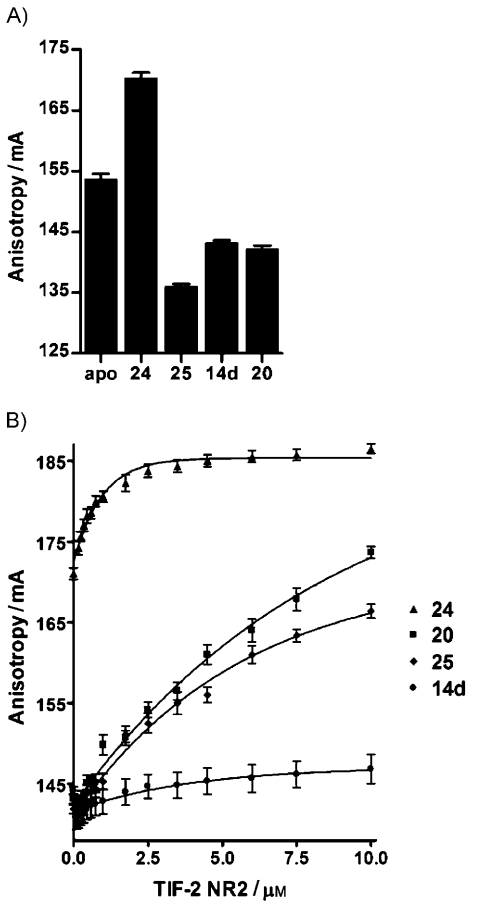

Figure 3. Ligand-induced RXRα helix H12 dynamics monitored by fluorescence anisotropy. A) Anisotropy values in the presence of saturating concentrations of the series of mixed agonists/antagonists **20** and **14d**. For comparison, we also measured the effect of the full-RXR agonist CD3254 (compound **24**) and the previously reported full antagonist UVI3003 **25**. B) Similar experiments were carried out in the presence of increasing concentrations of the NR interaction motif 2 peptide of the coactivator TIF2.

groups of the retinoid skeleton. By taking advantage of the availability of regioisomeric dihalogenated pyrazines, we were able to synthesize positional isomers of the arotinoids that have a different overall shape to guide the alternative targeting of RAR (pyrazine C3 and C6 connections) or RXR (pyrazine C3 and C5 connections). In addition, the C2 position of the pyrazine ring was functionalized with ether or amine groups. Through modification of the size and length of these groups, we expected to be able to modulate the activities of the retinoid receptors. The straightforward synthesis of the pyrazine arotinoids was based on sequential and halogen-selective palladium-catalyzed cross-coupling reactions.[20] Benzoic and acrylic acids were incorporated to a monohalogenated pyrazine after replacement of the more reactive halide by the hydrophobic tetrahydro-tetramethylnaphthalene ring by using a Suzuki coupling.

One of the most important outcomes of this study is the finding that some pyrazine-based arotinoids are potent RARα,β inverse agonists, in particular the acrylic acid derivatives (**14a–e**). **14c** showed the greatest discrimination in favor of RARβ while keeping the same affinity for RARα and RARβ. For the bent structures, a gain of RXR binding is generally observed. Compound **20**, which has an amine substituent, is a pan-RAR agonist with some RARβ selectivity and a low-affinity RXR antagonist, whereas pyrazine arotinoid **23** is active on RARs and RXR. Pyrazine acrylic acid with an isoamyl ether chain **14d** showed the unexpected property of being an inverse agonist also for RXR. This is an interesting observation because in contrast to RAR, the H12 helix of RXR masks corepressor access.[52] Provided that the basis of RXR inverse agonism is linked to increased corepressor interaction, this result implies that **14d** exerts an allosteric effect on RXR H12, which allows for a corepressor interaction.

Fluorescence anisotropy studies of a heterodimer containing the LBD of both RARα and RXRα with a fluorescein label attached to the C-terminal (H12) region of RXRα was used to monitor ligand-induced RXRα helix H12 dynamics. Consistent with the transactivation assays, compound **20** was characterized as a weak antagonist because the induced fluorescence anisotropy decreased relative to the full agonist CD3254 (**24**) [albeit moderately compared to the full antagonist UVI3003 (**25**)], but increased in the presence of the TIF-2 NR2 peptide. Compound **14d** showed the same reduced fluorescence anisotropy values as **20**, but these were not significantly increased by addition of the TIF2 coactivator peptide.

Conclusions

Potent inverse agonists based on a central pyrazine "linchpin" unit that exhibit selectivity for the RARα and RARβ subtypes have been discovered.[53] Structural modifications within the family of analogues can provide a gain of selectivity for RARβ, as shown by the replacement of a methyl by an ethyl group at the alkyl aryl ether (compounds **14a** and **14b**). Moreover, the pyrazine acrylic acid **14d** displays the unusual profile of a dual RARα,β/RXR inverse agonist. These are the first RAR (and RXR) inverse agonists with structural modifications at a central heterocyclic core. From a mechanistic standpoint, our studies reveal that the inverse agonism of **14d** and **14e** is due to the stabilization of the RAR complexes with the corepressors NCoR and SMRT. Although dissimilar in structure, it is conceivable that the alkyl/benzyl substituents of the pyrazine arotinoids **14a–e** are oriented towards the same region of the RAR ligand-binding domain than the aryl (**26**) and phenylethynyl (**27**) substituents of the previously described inverse agonists. Efforts towards the structural characterization of inverse agonists/retinoid receptor complexes to derive general principles of inverse agonism are underway.

Experimental Section

Cell lines, cell cultures and transactivation assays: The activity of the synthesized ligands has been measured in transactivation assays in two complementary systems. Both systems are based on fusion proteins, which consist of the ligand-binding domain of the corresponding receptor and the DNA-binding domain of either the human estrogen receptor (ER DBD) or the yeast GAL4 transcription factor. The cells also contain stably integrated luciferase reporters

controlled by estrogen responsive elements (for ER DBD chimeras) or five GAL4 response elements (for GAL4 DBD chimeras) in front of a minimal β-globin promoter; these are referred to as "ERE–βGlob-Luc-SV-Neo" or "(17 m)$_5$-βG-Luc".[36,54]

The cells were seeded into 96-well plates at a rate of 10000 cells per well in 100 μL Dulbecco's Modified Eagle Medium (DMEM) without phenol red and supplemented with 10% of defatted calf serum. The plates were then incubated at 37 °C and 7% CO_2 for 4 h.

For the "ERE–βGlob-Luc-SV-Neo" system the various dilutions of test compounds and reference ligands (ref. 100% (CD0193 100 nM); ref. 0% (CD4899 500 nM)) were added in a volume of 5 μL per well. Plates were then incubated at 37 °C, 7% CO_2. The culture medium was removed by turning over and a 1:1 PBS/luciferin reagent (100 μL) was added to each well. After 5 min, the plates were read by using the luminescence reader Microbeta Trilux (Wallac, Perkin Elmer, Courtaboeuf, France). To determine KdA and KdR, "crossed curves" of the test product against a reference agonist were performed in 96-well plates. The test product was used at ten concentrations and the reference agonist at seven concentrations. In each well, the cells were in contact with a concentration of the test product and a concentration of the reference agonist. The experimental crossed curves were compared to theoretical curves that were obtained by modelling the mathematical equations governing the equilibrium between the two receptor states in the presence of the two ligands:

$$\text{Signal} = \text{Bkg} + \text{Max}/(1 + ((1 + (L_0 \times \frac{1 + \frac{X_1}{K_{dR_1}} + \frac{X_2}{K_{dR_2}}}{1 + \frac{X_1}{K_{dA_1}} + \frac{X_2}{K_{dA_2}}}))/\frac{[R_{tot}]}{K_{deff}})^n)$$

where L_0 was the ratio of the receptor in resting state and active state in the absence of the ligand ([R]/[A]). Bkg was the background signal that corresponds to the signal (theoretical) in the absence of active receptor. To experimentally approach the value, the background signal at saturating dose of inverse agonist was used. Max was the maximum response that corresponds to the state where all receptors are in active state (theoretical). To experimentally approach the value, the response at saturating dose of full agonist was used; $X_{1(or\ 2)}$ was the concentration of ligand 1 (or 2); $K_{dR_{1(or\ 2)}}$ was the dissociation constant of ligand 1 (or 2) for the resting state; $K_{dA_{1(or\ 2)}}$ was the dissociation constant of ligand 1 (or 2) for the active state; n was an empirical power factor; $[R_{tot}]$ was the concentration of receptor in total; and K_{deff} was the dissociation constant of the effector. The following parameters were used: RARα: $L_0 = 500$, $[R_{tot}]/K_{deff} = 15$, $n = 1$; RARβ: $L_0 = 350$, $[R_{tot}]/K_{deff} = 15$, $n = 1$; RARγ: $L_0 = 70$, $[R_{tot}]/K_{deff} = 15$, $n = 1$; and RXR: $L_0 = 600$ $[R_{tot}]/K_{deff} = 15$, $n = 1$. The K_{dA} and K_{dR} values of the ligand of interest are a result of the best fit between experimental and theoretical curves. The K_{dapp} corresponds to the AC_{50}/IC_{50} value of the theoretically modeled curve of the product of interest in the absence of reference compound, with the exception of full antagonists, where $K_{dA} = K_{dR} = K_{dapp}$. Because the theoretically modeled curves were determined by curve-fitting based on all the experimental data of the crossed curves experiments (70 data points), the K_{dapp} and K_{dA}/K_{dR} values more precisely represented the real values than classical AC_{50}/IC_{50} values that were determined based on a single dose–response curve.

The effects of the described retinoids on RARα, RARβ, RARγ, and RXRα-mediated transactivation was confirmed by using a related reporter assay based on the generation of a fusion protein, which consisted of the ligand-binding domain of the corresponding receptor and the DNA-binding domain of the yeast GAL4 transcription factor. The cells also contained a stably integrated luciferase reporter, which was controlled by five GAL4 response elements in front of a β-globin promoter and this was termed "(17 m)$_5$-βG-Luc".

Two-hybrid assays: GAL-SMRT and GAL-NCoR have been previously described.[36] VP16-hRARα(DEF) and VP16- hRARβ(DEF) plasmids correspond to a fusion between the activation domain VP16 and residues 153 to 448 of hRARα, and residues 146 to 462 of hRARβ, respectively. For two-hybrid assays, 1.2×10^5 HeLa cells were seeded in 24-well plates. After attachment, cells were cotransfected with GAL4 chimera (50 ng), VP16 chimera (40 ng), (17mer)5×-βglob-luc (200 ng), and CMV-βGAL (50 ng), according to the jet-PEI™ (Polyplus Transfection, New York, USA) protocol. After 18 h, cells were treated with vehicle or ligand at 1 μM. After a further 16 h, cells were lysed in 1× passive lysis buffer (Promega, Charbonnières-les-Bains, France). Reporter gene activity was analyzed with a standard protocol for the luciferase assay and quantified by using a luminometer from Berthold Technologies (Bad Wildbad, Germany). The results were normalized to the β-galactosidase activities.

Steady-state fluorescence anisotropy: The RARα-RXRα LBD fluorescent heterodimer was prepared as previously described.[37] Fluorescence anisotropy assays were performed by using a Safire^2 microplate reader (TECAN, Lyon, France) at a protein concentration of 0.117 μM in buffer A (10 mM Tris-HCl, pH 8.0, 150 mM NaCl, 5 mM DTT, 1 mM EDTA, 10% glycerol). The excitation wavelength was set at 470 nm, and emission was measured at 530 nm. The TIF-2 NR2 coactivator peptide (686-KHKILHRLLQDSS-698, final concentration of 10 μM) was added to protein samples containing ligand (10 μM), and then the sample was diluted successively with buffer A that was supplemented with heterodimer (0.117 μM) and ligand (10 μM). At least three independent measurements were made for each sample.

Acknowledgements

The authors are grateful to the European Union (Anticancer Retinoids, QLK3-2002-02029), the MEC-Spain (SAF2004-07131; SAF2007-63880-FEDER), Xunta de Galicia (grant 08CSA052383PR from DXI+D+i; Consolidación 2006/15 from DXPCTSUG), the INCa, the ANR and the Ligue National Contre le Cancer (H.G., équipe labelisé) for financial support.

Keywords: arotinoids · heterocycles · nuclear hormone receptors · retinoid receptors · structure–activity relationships

[1] P. Germain, P. Chambon, G. Eichele, R. M. Evans, M. A. Lazar, M. Leid, A. R. de Lera, R. Lotan, D. J. Mangelsdorf, H. Gronemeyer, *Pharmacol. Rev.* **2006**, *58*, 712–725.
[2] P. Germain, P. Chambon, G. Eichele, R. M. Evans, M. A. Lazar, M. Leid, A. R. de Lera, R. Lotan, D. J. Mangelsdorf, H. Gronemeyer, *Pharmacol. Rev.* **2006**, *58*, 760–772.
[3] V. Laudet, H. Gronemeyer, *The Nuclear Receptor Facts Book*; Academic Press, San Diego, **2002**.
[4] M. Mark, N. Ghyselinck, P. Chambon, *Annu. Rev. Pharmacol. Toxicol.* **2006**, *46*, 451–480.
[5] L. Altucci, H. Gronemeyer, *Nat. Rev. Cancer* **2001**, *1*, 181–193.
[6] L. Altucci, M. D. Leibowitz, K. M. Ogilvie, A. R. de Lera, H. Gronemeyer, *Nat. Rev. Drug Discovery* **2007**, *6*, 793–810.
[7] A. I. Shulman, D. J. Mangelsdorf, *N. Engl. J. Med.* **2005**, *353*, 604–615.
[8] A. Chawla, Y. J. Repa, R. M. Evans, D. J. Mangelsdorf, *Science* **2001**, *294*, 1866–1870.

[9] J. J. Repa, D. J. Mangelsdorf, *Nat. Med.* **2002**, *8*, 1243–1248.
[10] B. P. Klaholz, J.-P. Renaud, A. Mitschler, C. Zusi, P. Chambon, H. Gronemeyer, D. Moras, *Nat. Struct. Biol.* **1998**, *5*, 199–202.
[11] W. Bourguet, M. Ruff, P. Chambon, H. Gronemeyer, D. Moras, *Nature* **1995**, *375*, 377–382.
[12] A. R. de Lera, W. Bourguet, L. Altucci, H. Gronemeyer, *Nat. Rev. Drug. Discovery* **2007**, *6*, 811–820.
[13] P. Loeliger, W. Bollag, H. Mayer, *Eur. J. Med. Chem.* **1980**, *15*, 9–15.
[14] M. I. Dawson, L. Jong, P. D. Hobbs, D. Xiao, K.-C. Feng, W.-R. Chao, C. Pan, J. A. Fontana, X.-k. Zhang, *Bioorg. Med. Chem. Lett.* **2000**, *10*, 1311–1313.
[15] A. Dhar, S. Liu, J. Klucik, K. D. Berlin, M. M. Madler, S. Lu, R. T. Ivey, D. Zacheis, C. W. Brown, E. C. Nelson, P. J. Birkbichler, D. M. Benbrook, *J. Med. Chem.* **1999**, *42*, 3602–3614.
[16] D. Simoni, M. Roberti, F. P. Invidiata, R. Rondanin, R. Baruchello, C. Malagutti, A. Mazzali, M. Rossi, S. Grimaudo, F. Capone, L. Dusonchet, M. V. Raimondi, M. Landino, N. D'Alessandro, M. Tolomeo, D. Arindam, S. Lu, D. M. Benbrook, *J. Med. Chem.* **2001**, *44*, 2308–2318.
[17] D. L. Gernert, D. A. Neel, M. F. Boehm, M. D. Leibowitz, D. E. Mais, P. Y. Michellys, D. Rungta, A. Reifer-Miller, T. A. Grese, *Bioorg. Med. Chem. Lett.* **2004**, *14*, 2759–2763.
[18] C. D. Haffner, J. M. Lenhard, A. B. Miller, D. L. McDougald, K. Dwornik, O. R. Ittoop, R. T. Gampe, H. E. Xu, S. Blanchard, V. G. Montana, T. G. Consler, R. K. Bledsoe, A. Ayscue, D. Croom, *J. Med. Chem.* **2004**, *47*, 2010–2029.
[19] J. Sakaki, M. Kishida, K. Konishi, H. Gunji, A. Toyao, Y. Matsumoto, T. Kanazawa, H. Uchiyama, H. Fukaya, H. Mitani, Y. Arai, M. Kimura, *Bioorg. Med. Chem. Lett.* **2007**, *17*, 4804–4807.
[20] *Metal-Catalyzed Cross-Coupling Reactions*, 2nd. ed. (Eds.: A. de Meijere, F. Diederich), Wiley-VCH, Weinheim, **2004**.
[21] E. L. Ghisalberti, C. H. Hocart, P. R. Jefferies, G. M. Proudfoot, B. W. Skelton, A. H. White, *Aust. J. Chem.* **1983**, *36*, 993–1000.
[22] N. K. Garg, R. Sarpong, B. M. Stoltz, *J. Am. Chem. Soc.* **2002**, *124*, 13179–13184.
[23] K. Pieterse, A. Lauritsen, A. P. H. J. Schenning, J. A. J. M. Vekemans, E. W. Meijer, *Chem. Eur. J.* **2003**, *9*, 5597–5604.
[24] N. K. Garg, B. M. Stoltz, *Tetrahedron Lett.* **2005**, *46*, 2423–2426.
[25] R. J. Huntley, R. L. Funk, *Org. Lett.* **2006**, *8*, 4775–4778.
[26] H. Nakamura, D. Takeuchi, A. Murai, *Synlett* **1995**, 1227–1228.
[27] T. Jeffery, *Tetrahedron* **1996**, *52*, 10113–10130.
[28] N. E. Leadbeater, M. Marco, *Org. Lett.* **2002**, *4*, 2973–2976.
[29] N. E. Leadbeater, M. Marco, *J. Org. Chem.* **2003**, *68*, 888–892.
[30] H. Nakamura, M. Aizawa, D. Takeuchi, A. Murai, O. Shimoura, *Tetrahedron Lett.* **2000**, *41*, 2185–2188.
[31] B. Jiang, C.-G. Yang, W.-N. Xiong, J. Wang, *Bioorg. Med. Chem.* **2001**, *9*, 1149–1154.
[32] M. J. Reyes, R. Castillo, M. L. Izquierdo, J. Alvarez-Builla, *Tetrahedron Lett.* **2006**, *47*, 6457–6460.
[33] J. Y. Chen, S. Penco, J. Ostrowski, P. Balaguer, M. Pons, J. E. Starrett, P. Reczek, P. Chambon, H. Gronemeyer, *EMBO J.* **1995**, *14*, 1187–1197.
[34] J. Monod, J. Wyman, J. P. Changeux, *J. Mol. Biol.* **1965**, *12*, 88–118.
[35] T. P. Kenakin, *Recept. Channels* **2001**, *7*, 371–385.
[36] P. Germain, J. Iyer, C. Zechel, H. Gronemeyer, *Nature* **2002**, *415*, 187–192.
[37] V. Nahoum, E. Pérez, P. Germain, F. Rodríguez-Barrios, F. Manzo, S. Kammerer, G. Lemaire, O. Hirsch, C. A. Royer, H. Gronemeyer, A. R. de Lera, W. Bourguet, *Proc. Natl. Acad. Sci. USA* **2007**, *104*, 17323–17328.
[38] V. Pogenberg, J.-F. Guichou, V. Vivat-Hannah, S. Kammerer, E. Pérez, P. Germain, A. R. de Lera, H. Gronemeyer, C. A. Royer, W. Bourguet, *J. Biol. Chem.* **2005**, *280*, 1625–1633.
[39] E. S. Klein, M. E. Pino, A. T. Johnson, P. J. A. Davies, S. Nagpal, S. M. Thacher, G. Krasinski, R. A. S. Chandraratna, *J. Biol. Chem.* **1996**, *271*, 22692–22696.
[40] H. Gronemeyer, J.-A. Gustafsson, V. Laudet, *Nat. Rev. Drug Discovery* **2004**, *3*, 950–964.
[41] L. Nagy, H. Y. Kao, J. D. Love, C. Li, E. Banayo, J. T. Gooch, V. Krishna, K. Chatterjee, R. M. Evans, J. W. Schwabe, *Genes Dev.* **1999**, *13*, 3209–3216.
[42] V. Perissi, L. M. Staszewski, E. M. McInerney, R. Kurokawa, A. Krones, D. W. Rose, M. H. Lambert, M. V. Milburn, C. K. Glass, M. G. Rosenfeld, *Genes Dev.* **1999**, *13*, 3198–3208.
[43] O. Hermanson, C. K. Glass, M. G. Rosenfeld, *Trends Endocrinol. Metab.* **2002**, *13*, 55–60.
[44] K. Jepsen, O. Hermanson, T. M. Onami, A. S. Gleiberman, V. Lunyak, R. J. McEvilly, R. Kurokawa, V. Kumar, F. Liu, E. Seto, S. M. Hedrick, G. Mandel, C. K. Glass, D. W. Rose, M. G. Rosenfeld, *Cell* **2000**, *102*, 753–763.
[45] N. J. McKenna, B. W. O'Malley, *Cell* **2002**, *108*, 465–474.
[46] C. L. Smith, B. W. O'Malley, *Endocr. Rev.* **2004**, *25*, 45–71.
[47] X. Hu, M. A. Lazar, *Nature* **1999**, *402*, 93–96.
[48] M. I. Dawson, *Curr. Med. Chem. Anti-Cancer Agents* **2004**, *4*, 199–230.
[49] M. Gèhin, V. Vivat, J.-M. Wurtz, R. Losson, P. Chambon, D. Moras, H. Gronemeyer, *Chem. Biol.* **1999**, *6*, 519–529.
[50] W. Bourguet, V. Vivat, J.-M. Wurtz, P. Chambon, H. Gronemeyer, D. Moras, *Mol. Cell* **2000**, *5*, 289–298.
[51] W. Bourguet, P. Germain, H. Gronemeyer, *Trends Pharmacol. Sci.* **2000**, *21*, 381–388.
[52] J. Zhang, X. Hu, M. A. Lazar, *Mol. Cell. Biol.* **1999**, *19*, 6448–6457.
[53] Arotinoids with pyrazine rings in the hydrophobic terminus and a pyrrole as central unit have been described: K. Kikuchi, S. Hibi, H. Yoshimura, K. Tai, T. Hida, N. Tokuhara, T. Yamauchi, M. Nagai, *Bioorg. Med. Chem. Lett.* **2000**, *10*, 619–622.
[54] V. Vivat, C. Zechel, J.-M. Wurtz, W. Bourguet, H. Kagechika, H. Umemiya, K. Shudo, D. Moras, H. Gronemeyer, P. Chambon, *EMBO J.* **1997**, *16*, 5697–5709.

Received: January 19, 2009
Published online on April 2, 2009

